33RD INTERNATIONAL COSMIC RAY CONFERENCE, RIO DE JANEIRO 2013
THE ASTROPARTICLE PHYSICS CONFERENCE

ICRC 2013

Following solar activity with CaLMa

JUAN JOSÉ BLANCO[1,2], RAÚL GÓMEZ-HERRERO[1,2], JOSÉ MEDINA[1,2], EDWIN CATALÁN[2], ÓSCAR GARCÍA[1,2], IGNACIO GARCÍA[1,2]

[1] *SRG- Universidad de Alcalá (Spain)*
[2] *SRG-CaLMa*

juanjo.blanco@uah.es

Abstract: The Castilla-La Mancha (CaLMa) neutron monitor is continuously operating since 26 October 2011. It is located at Guadalajara (40°38'N, 3°9'W) at 708 m above sea level and 55 km away from Madrid. It is covering a gap in the Neutron Monitor Data Base (NMDB), thanks to its geographical location, its height above sea level and its vertical cutoff rigidity (6.95 GV). CaLMa is providing counts of galactic cosmic rays (GCRs) with a temporal resolution of 1 min, being the mean count rate 5 c/s/counter. This high cadence allows the monitoring of solar activity by mean the observed variation in count rate. Both in the sort term and in the long term activity, i.e., flare or coronal mass ejections and solar modulation, can therefore be studied with CaLMa's measurements. During this last year, CaLMa has measured variations in the GCR count rate related to interplanetary coronal mass ejections, fast solar wind streams, shocks and stream interaction regions. In this work we analyze the solar wind condition associated to variations in CaLMa's count rate and we compare them with other neutron monitors.

Keywords: Neutron monitor, cosmic rays, solar energetic particles, solar activity.

1 Introduction

As it has been commented in the abstract, CaLMa is the new neutron monitor (NM) of Castilla-La Mancha located in Guadalajara (Spain, 40°38'N, 3°9'W at 708 m above sea level and 6.95 GV). CaLMa is the first NM installed in Spain and it is covering a previous gap in the neutron monitor data base [1]. It is composed by 15 $^{10}BF_3$ counters, three of them are the old BP28 model and the remaining twelve are a new LND2061 model. The main characteristics of these new tubes are described in [2]. CaLMa has gone through different stages. Its operation started on October 26th, 2011 with three BP28 tubes (3 NM64), three LND2061 tubes were added on March 27th, 2012 (6 NM64), afterwards three LND2061 tubes were incorporated on June 22, 2012 (9 NM64), two LND2061 tubes were added on June 26th, 2012 (11 NM64), and finally, four LND2061 tubes completed the station on July 11th. It is fully operative since July 2012 (15 NM64) [2], providing 1 minute data in real time. Its measurements can be plotted and downloaded at http://www.nmdb.eu/nest/search.php. A more detailed information about CaLMa can be found in http://www.calmanm.es/.

Neutron monitors measure GCRs and solar energetic particles (SEPs) in the range between 1 GeV and 20 GeV. SEPs in this energy range are relativistic and arrived to Earth in the order of 30 min before the main bulk of SEPs with energies about 1 MeV/n, which are the most dangerous component of SEPs for satellites and human life. This makes neutron monitors key detectors in a global network of space weather alert system [3].

Because of its vertical rigidity cut-off (6.95 GV), CaLMa is able to monitor the flux of galactic cosmic rays (GCRs) with energies higher than 6.07 GeV/n. These GCRs are strongly modulated by the solar activity and variations in their flux let to follow the solar activity along the solar cycle. These variations can be increases known as ground level enhancements (GLEs) [4] and reductions termed as Forbush decreases (FDs) [5]. A FD is often produced by the passage of an interplanetary coronal mass ejection (ICME), i. e. the interplanetary counterpart of coronal mass ejections (CMEs), that can be accompanied by an embedded magnetic cloud (MC) [6] and their driven shock. Here, we assume the definition of MC given by Burlaga [7], as a solar wind region with relative high magnetic field, soft magnetic field rotation and low temperature. Stream interaction regions (SIR), i.e. the surface between slow solar wind streams and fast solar wind streams, with their associated forward and reversal shocks can be also effective FD producers [8].

In this work, we present the first measures taken from CaLMa and its response to solar wind structures as SIRs, ICMEs and interplanetary shocks.

2 Data analysis

Variations in NM count rate background are mainly due to solar activity, Earth rotation and NM malfunction. CaLMa malfunctions are recorded and flagged, if they happen, into the CaLMa database. Nevertheless, daily variation has to be determined to distinguish between variations due to solar activity and Earth rotation effects. To determine this variation, a period free of solar activity has been selected from CaLMa database (figure1). CaLMa count rate has to be pressure corrected to remove the effect of variations in the air column thickness along the secondary particle path. The pressure measured during this period is presented in the upper panel of figure 1 and the uncorrected count rate is shown in bottom panel of figure 1. Once the period has been selected and count rate is pressure corrected, CaLMa count rate has been fitted to a sinusoidal function to confirm and visualize the GCR flux daily dependence (24 h period) in this period of data (continuous black line in mid-

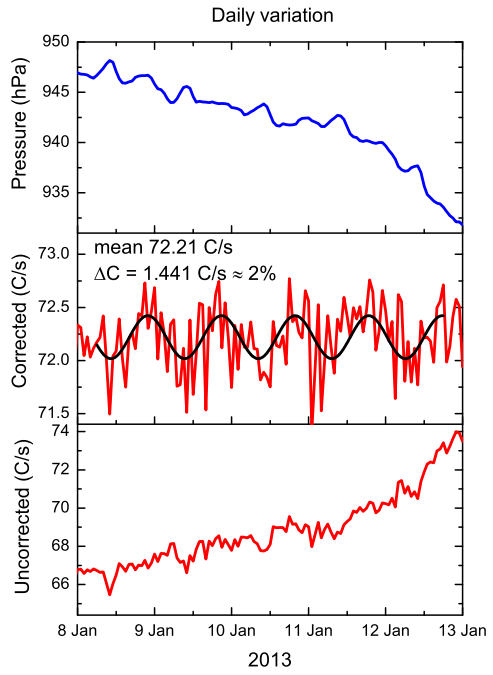

Figure 1: CaLMa corrected count rate and sinusoidal fit function, red and black line respectively (middle panel) uncorrected count rate (bottom panel)and pressure (upper panel)

dle panel of figure 1. It is readily observed how GCR count rate is affected by Earth rotation. A variation of 2 % in count rate has been estimated as caused by this daily period. This value has been computed by subtracting between the maximum and minimum count rate measured during this interval.

Hourly averaged data of CaLMa count rate have been analysed from October 20th, 2011 to April 30th, 2013 with the goal to determine the CaLMa response to variations in solar wind and solar activity. The magnetospheric response has been also compared with the CaLMa measurements. Hourly OMNI data provided by OMNIWeb service have been used to analyse solar wind conditions near Earth and the magnetospheric response by means of solar wind density, temperature, speed, magnetic field, Dst index and Kp index. These measurements have been compared with those provided by CaLMa.

3 Results

CaLMa has observed thirteenth FDs (Table 1) since October 2011. A decrease in the count rate is catalogued as FD if the decrease in amplitude is higher than the amplitude of the daily variations in the count rate. All of them have been also observed by other NMs in the NMDB. These FDs had decrease percentages ranged between 1.9% and 8.92%. All of them showed decreases higher than 2%, i. e. possible daily variations are discarded with this threshold, except in two events. They were included into the list of FD detected by CaLMa because both were clearly observed by other NM stations. The time of each event in table 1 correspond with the minimum in the CaLMa count rate for that event.

Event	Date	FD	gmtorm
sh+MC+SIR	24/01/2012 23:59	2.34	Yes
sh+MC+sh+MC	08/03/2012 22:38	8.92	Yes
sh+MC	13/03/2012 06:38	3.05	No
MC	06/04/2012 01:38	4.66	No
sh+SIR+MC	26/04/2012 13:38	1.94	Yes
sh+MC	17/06/2012 00:00	3.05	Yes
sh+MC	14/07/2012 16:00	3.05	Yes
sh+MC+MC	05/09/2012 03:00	2.88	Yes
sh+MC	13/11/2012 15:00	3.64	Yes
sh+MC + SIR	24/11/2012 23:00	3.26	No
MC	17/01/2013 13:00	1.9	No
sh+SIR+sh+MC	18/03/2013 20:00	5.1	Yes
sh+MC	14/04/2013 18:00	3.74	No

Table 1: FDs observed by CaLMa from December 2011 to April 2013. gmtorm = geomagnetic storm and sh = shock

An interplanetary shock was detected in eleven of the thirteen FDs. The two events without shock were observed during a MC passage. MCs were observed in all the events. Interplanetary shocks with MCs were detected in five cases. Isolated SIRs could not be associated with FDs. Combinations of more than two structures, i.e. interplanetary shock, MC and SIR, produced observable FDs by CaLMa in five events. Nevertheless, a relationship between the complexity of the solar wind environment and the depth of the FDs has not been found. A direct conclusion is that MCs play a central role as trigger of the FDs observed by CaLMa.

As for the magnetospheric response, a strong geomagnetic disturbance was observed in seven cases. Here strong means a Dst less than -75 nT, nevertheless, the minimum in the FD does not coincide with the minimum in Dst index being, in most of the events, clearly shifted one with respect to the other. It is clear from Table 1 that common drivers of Dst storms as SIRs [9], are not so effective in producing FDs as in producing Dst geomagnetic storms.

Examples of FDs observed by CaLMa and the lack of CaLMa's response to the GLE71 are analysed in the following subsections.

3.1 CaLMa's FD examples

CalMa observed the deepest FD (8.92%) on March 8th, 2012. The CaLMa count rate showed a relative long main phase (about two days) and long recovery phase (about fourteen days). During the recovery phase, a second FD happened on March 13th (see upper panel in figure 2). It can be said that this was a complex event in terms of the observed GCR flux.

As for the magnetospheric response, it was also a complex event with at least three geomagnetic storms. Only the most intense storm happened in coincidence with the first and deepest FD (second and third panels in figure 2) but the minimum in the CaLMa count rate is about two hours shifted with respect the minimum in the Dst index.

The solar wind conditions were very complex, with several solar wind structures sweeping up the Earth orbit. On March 7th a interplanetary shock was detected followed by a turbulent magnetic field region and an increase in the so-

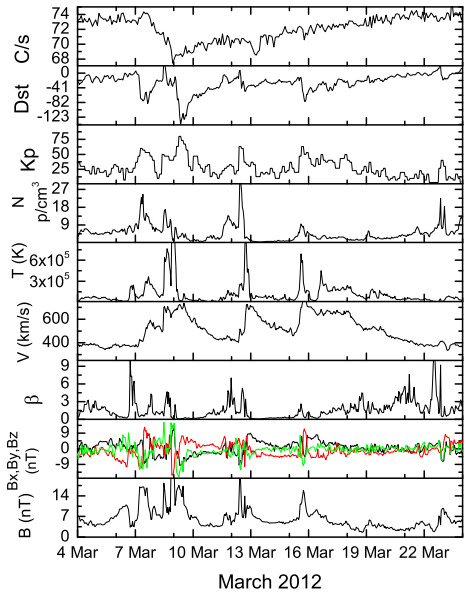

Figure 2: Complex FD event observed by CaLMa. From top to bottom CaLMa count rate, Dst index, Kp index, solar wind density, temperature and speed, plasma beta, magnetic field components and field intensity at 1 AU.

lar wind speed of more than 200 km/s. Although no effect was observed in CaLMa, a moderate geomagnetic storm was detected. A second shock driven by a MC arrived one day later. The shock and the MC triggered a deep FD with a decrease of about 8.92% with respect to the unperturbed region previous to the FD. A strong geomagnetic storm developed in coincidence with the MC arrival and a large Bz variation (green line in eighth panel in figure 2). Both recovery phases, i.e. FD and geomagnetic storm, began during the MC passage but the recovery to unperturbed levels in Dst index was faster than in the neutron monitor count rate.

A second FD was observed during the recovery phase four days later along with a third shock and a MC passage. A weak magnetospheric response was appreciated in this event. Nevertheless a large solar wind speed variation (more than 200 km/s) with a jump in temperature and density was also detected.

Three days later, a moderate geomagnetic storm was initiated by a shock driven by a SIR but no evidences of a MC passage were observed, and no count rate variations were detected in CaLMa neither.

From this example, it seems clear the complex relationship between magnetospheric response a GCR decreases if exist. The same structures can produce geomagnetic storm and FD but the involved mechanism seems to be different. GCR propagation conditions are affected mainly by the shock strength, the existence of turbulence and the MC size, the speed and magnetic field magnitude while the magnetosphere is affected by fast Bz component variations.

An example of single FD observed by CaLMa is shown in figure 3. The count rate was reduced by a 3.05%. This FD had a quite symmetric shape and short. It lasted hardly 24 hours. A shock arrived at 1 AU on June 16th followed by a MC ten hours later. The FD minimum was achieved on June 17th with the MC arrival. The shock did not produce any effect on CaLMa count rate, being the MC sheath what produced the FD main phase. Dst and Kp index showed a different behaviour. An abrupt increase in the Kp index was registered at the same time that the shock was detected. It reached its maximum with the MC sheath arrival and the starting time of the FD. A Dst storm begun after two hours the minimum in the count rate was reached. Its recovery phase begun after the FD recovery phase had finished.

This example seems to confirm the different nature of the responsible mechanism of the GCR decrease and the geomagnetic storm.

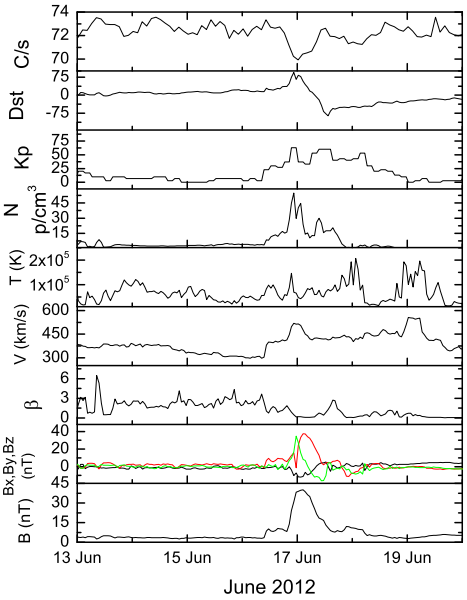

Figure 3: Single FD event observed by CaLMa. From top to bottom CaLMa count rate, Dst index, Kp index, solar wind density, temperature and speed, plasma beta, magnetic field components and field intensity at 1 AU.

3.2 GLE 71

The first solar cycle 24 ground level event (GLE 71) was detected on May 17th, 2012, by the NM global network (figure 4). It was observed by stations located at rigidities below 2.36 GV. Because of this rigidity cut-off, CaLMa did not observe any enhancement in its count rate. Other NM at similar rigidities did not observe it neither (see count rate plots of Rome and Jungfraujoch, blue and red lines respectively, in figure 4).

It seems to have the two components as can be noted in South Pole neutron monitor count rate (black line in figure 4). The prompt component is quite symmetric with an abrupt rise phase and fast decaying phase. This prompt component lasted less than one hour. The gradual component rise phase is masked by the prompt component and the decay phase lasted almost three hours. This behaviour

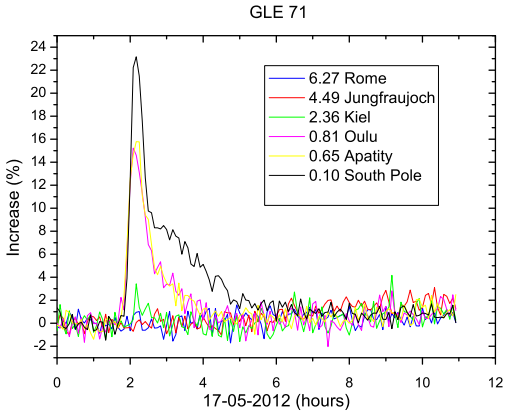

Figure 4: GLE 71 as observed by six stations into the NMDB. Arranged from higher to lower rigidity, Rome, Jungfraujoch, Kiel, Oulu, Apatity and South pole. Blue, red, green pink, yellow and black lines respectively.

is similar to those described in McCracken et al., [10] for their selection of the most intense GLEs.

Regarding to this GLE 71, Gopalswamy et al. [11] mark as a possible solar source of this event, a moderate flare (M5.1) and a fast CME with a well developed shock ahead. They conclude that the driven shock plays the main role in producing the GLE particles, especially if they are well connected with the shock nose. The response to rigidities lower than 2.36 GV could be explained if the shock is the main source of the accelerated particles in this event. On the other hand, the prompt component could be explained as a result of a good magnetic connection between the shock nose and the Earth, and the gradual component could be explained if these particles come from other regions apart of the shock nose.

4 Conclusions

The main conclusions about CaLMa status and measurements after eighteen months of operation can be itemized as:

- CaLMa is working since end of October 2011. It is providing one minute measurements of GCRs with energies higher than 6.07 GeV/n arriving to the Earth. It is composed by 15 $^{10}BF_3$ counters following the NM64 standard and it is integrated into the Neutron Monitor Data Base [1].
- CaLMa has detected thirteen FD with decreases higher than 2% in clear association with solar wind structures arriving to the Earth orbit. This fact confirms the adequate response of CaLMa to changes in the GCR propagation conditions due to variation in solar activity.
- MCs seem to play a central role in producing FDs. Such structures are involved in all the FDs detected by CaLMa. Driven shocks play also a relevant role in eleven of thirteen FDs. Nevertheless, SIR as isolated structure are not able to produce FDs.
- Although geomagnetic storm were observed in coincidence with FDs in eight cases, the responsible mechanism of producing GCR decreases and the geomagnetic storms is different.
- CaLMa has not observed any enhancement in its count rate during the last ground level enhancement (GLE 71). It is expected that CaLMa will observe GLEs produced by solar energetic particles with rigidities higher than 6.95 GV.

As an early future work it is planned to incorporate a muon telescope to CaLMa. We expect to improve our statistics and to get better directional information with this action.

Acknowledgment: The authors would like to thank the OMNIweb team and the Neutron Data Base for the use of their data. This work has been supported by JCCM through the project PPII1001506529 and by Ministerio de Ciencia y Tecnologiá through the project AYA2011-29727-C02-01.

References

[1] H. Mavromichalaki et al., Adv. Space Res., 47 (2011) 2210-2222 doi:10.1016/j.asr.2010.02.019.
[2] J. Medina et al., Nuclear Instruments (2013) under revision
[3] T. Kuwabara, et al. , Space Weather, 4 (2006) S08001 doi:10.1029/2005SW000204.
[4] P. Meyer, E. N. Parker and J. A. Simpson, Physical Review 104 (1956) 768783 doi:10.1103/PhysRev.104.768.
[5] S.E. Forbush, Physical Review, 51 (1937) 1108-1109 doi:10.1103/PhysRev.51.1108.3.
[6] J.J. Blanco, et al., Solar Phys., 284 (2013) 167-178 doi: 10.1007/s11207-013-0256-1.
[7] L. F. Burlaga, E. Sittler, F. Mariani, and R. Schwenn, J. Geophys. Res., 86 (1981) 6673.
[8] I. G. Richardson, G. Wibberenz, and H. V. Cane, J. Geophys. Res., 101 (1996), 13483
[9] I. G. Richardson, H. V. Cane, J. Space Weather Space Clim., 2 (2012) A01
[10] K.G. McCracken, H. Moraal, M.A. Shea, Astrophys. J., 761 (2012) 101-112.
[11] N. Gopalswamy et al., Astrophys. J. Letters, 765 (2013) L30-L34.